3D TV-Based Compressed MR Image Reconstruction Using a Primal Dual Algorithm

Abolfazl Mehranian[1], Hamidreza Saligheh Rad[1,2], Mohammadreza Ay[1,2], and Arman Rahmim[3]

[1]Medical Physics and Biomedical Engineering Department, Tehran University of Medical Sciences of Medical Sciences, Tehran,Iran, Tehran, Tehran, Iran, [2]Research Center for Science and Technology in Medcine, Imam Hospital, Tehran, Tehran, Iran, [3]Department of Radiology, School of Medicine, Johns Hopkins University, Baltimore, Maryland, United States

Introduction

Emerging trends toward fast magnetic resonance (MR) imaging focus on partial Fourier measurements and *k*-space undersampling. However, undersampling inevitably violates the Nyquist sampling criterion, thereby Fourier reconstructions exhibit aliasing artifacts and reduced signal-to-noise ratio (SNR). By establishing a direct link between sampling and sparsity, compressed sensing (CS) has, however, made it possible to accurately reconstruct MR images from undersampled *k*-spaces [1]. In this study, we introduced a fast primal-dual (PD) algorithm for CS-MR image reconstruction using variable-density spiral trajectories. The algorithm was developed for 3D total variation (TV) and Huber regularizations and was found to be very efficient and promising for fast 3D MRI.

Materials and Methods

Image Acquisition: We performed CS-MRI in a cardiac dataset of size 128×128×30 (Fig. 1A) with 80% *k*-space undersampling using a stack of variable-density spiral trajectories and 40 dB complex additive Gaussian noise. In order to reconstruct this dataset, let us consider the following compressed MR acquisition model:

(1) $$y = \Phi\mathcal{F}x + w$$

where $y \in \mathbb{C}^M$ is the undersampled *k*-space of the original cardiac dataset $x \in \mathbb{R}^N$, contaminated with the additive noise w. $\mathcal{F} \in \mathbb{C}^{N\times N}$ is a unitary Fourier basis through which x is being sensed and $\Phi \in \mathbb{R}^{M\times N}$ is a binary sampling matrix that compresses (reduces) the frequency data to $M < N$ samples (sampling ratio: 0.20). One approach to recover x is by zero-filling the missing *k*-space samples in y followed by an inverse Fourier transform. As shown in Fig. 1B, this method, however, results in artifacts obscuring anatomical features and thus reduced SNR. The most efficient approach is however to reconstruct x by the following CS problem:

(2) $$\hat{x} = \mathrm{argmin}_x \frac{\lambda}{2}\|\Phi\mathcal{F}x - y\|^2 + \sum_i^N \varphi(|\nabla x|_i)$$

where the first term enforces data fidelity and the second, known as prior, promotes sparsity, and λ controls the balance between them. ∇ is a 3D gradient operator and φ is a potential function. For the TV and Huber sparsity-promoting priors, we define $\varphi_{TV}(t) = t$ and $\varphi_H(t) = t^2/2\alpha$ if $t < \alpha$ and $t - \alpha/2$ otherwise, where α reduces the staircasing effect of the TV prior. This CS approach in fact attempts to exploit the sparsity of the gradients of x to recover it from its undersampled *k*-space i.e. y.

Reconstruction algorithm: We recast the primal problem (2) into its corresponding primal-dual formulation as follows:

(3) $$\max_u\{\min_x\langle\nabla^* u, x\rangle + G(x)\} - F^*(u)$$

where ∇^* is the dual of the gradient operator, F^* is the dual of an ℓ^1-norm used in TV prior, and $G(x)$ is the first term in (2). To solve the above problem, we adopted the following algorithm proposed in [2] and solved its proximal maps, prox(·), for TV and Huber-based CS MRI

(4) $$\begin{aligned} u^{k+1} &= \mathrm{prox}_{\sigma F^*}(u^k + \sigma\nabla\bar{x}^k) \\ x^{k+1} &= \mathrm{prox}_{\tau G}(x^k - \tau\nabla^* u^{k+1}) \\ \bar{x}^{k+1} &= x^k + \theta(x^{k+1} - x^k) \end{aligned}$$

Proximal map of F^*. To solve this map, we make use of Moreau's identity [3], as well as the fact that the proximal map of an ℓ^1-norm is a point-wise soft thresholding. Thus, for a TV prior, we can derive $\mathrm{prox}_{\sigma F^*}(\tilde{u}) = \tilde{u}/\max\{1, |\tilde{u}|\}$. For a Huber prior, we make use of Lemma 2.6 in [3], we then derive its map as $\mathrm{prox}_{\sigma F_H^*}(\tilde{u}) = \mathrm{prox}_{\sigma F^*}(\tilde{u}/1 + \sigma\alpha)$.

Proximal map of G. To solve this map, we equate it first derivative to zero, thereby a linear system of equations is obtained. By making use of matrix inversion lemma and the fact that $\mathcal{F}\mathcal{F}^H = \mathcal{F}^H\mathcal{F} = I$ and $\Phi\Phi^T = I$, due to the special structure of Φ, and, we then derive the map as $\mathrm{prox}_{\tau G}(\tilde{x}) = \tilde{x} + (\tau\lambda/(1+\tau\lambda))\mathcal{F}^H\Phi^T(\mathrm{y} - \Phi\mathcal{F}\tilde{x})$.

Results and Conclusions

Fig. 1 compares the results of zero-filling reconstruction with those of the proposed primal-dual (PD) TV and Huber regularizations. Our algorithms sufficiently recover the original images and their diagnostically important details. As presented, the algorithms significantly improved the SNR in the reconstructed dataset. Fig 2A shows improvement in SNR for the algorithms versus computation time (CPU) in a 2.6 GHz PC. As seen, the Huber prior can achieve better SNR performance provided an appropriate parameter selection. It is also noticeable that the PD algorithm recovers the 3D MR images within ~20 seconds. We also compared this algorithm with the best case performance of three advanced algorithms, namely, split augmented Lagrangian shrinkage algorithm (SALSA) [4], forward-backward splitting (FBS) [3] and Douglas-Rachford Splitting (DRS) [5]. The results are shown in Fig 2B. As seen, the proposed PD algorithm is much faster than the other algorithms in SNR enhancement and hence in image reconstruction.

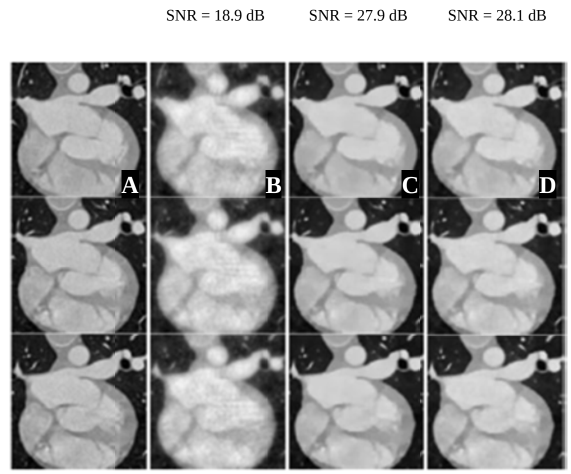

Figure 1. *Columns:* A) True image, B) Zero-filling C) TV and D) Huber regularizations. *Titles:* SNR after convergence.

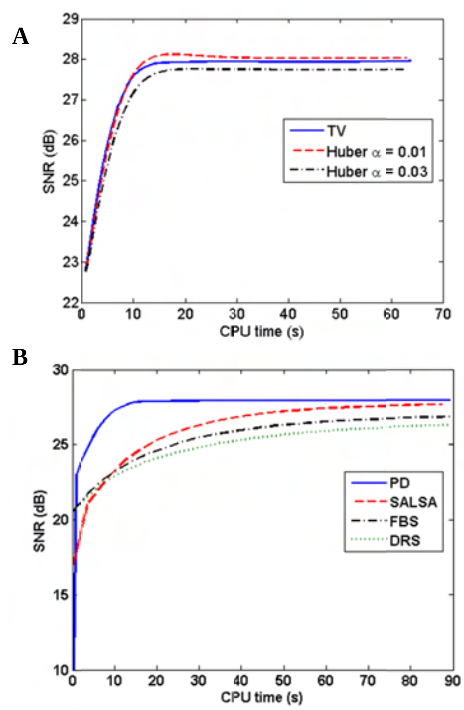

Figure 2. SNR vs. CPU time. A) TV and Huber regularizations. B) The SNR performance of the proposed PD vs. the other competing algorithms for TV regularization.

References

[1] Lustig M *et al*, *Magn. Reson. Med.*, 58, 1182-1195, 2007. **[2]** Chambolle A and Pock T, *J. Math Imaging Vis.*, 40(1): 120-145, 2010. **[3]** Combettes PL and Wajs VR, *SIAM Multi. Model Simul.*, 4(4): 1168-1200, 2005. **[4]** Afonso MV *et al*, *IEEE Trans. Im. Proc.*, 19(9): 2345-56, 2010. **[5]** Combettes PL and Pesquet JC, *IEEE J. Selected Topics Signal Proc.*, 1(4): 1-12, 2007.